

# Holographic Superconductors: An Analytic Method Revisit

En-Jui Chang,<sup>1,\*</sup> Chia-Jui Chou,<sup>1,†</sup> and Yi Yang<sup>1,‡</sup>

<sup>1</sup>*Department of Electrophysics, National Chiao Tung University, Hsinchu, ROC*

## Abstract

We study a non-minimal holographic superconductors model in both non-backreaction and full-backreaction cases using an analytic matching method. We calculate the condensate of the dilaton and the critical temperature of the phase transition. We also study the properties of the electric conductivity in various parameters.

arXiv:1812.04288v3 [hep-th] 8 Mar 2019

---

\*Electronic address: [phyenjui@gmail.com](mailto:phyenjui@gmail.com)

†Electronic address: [agoodmanjerry.ep02g@nctu.edu.tw](mailto:agoodmanjerry.ep02g@nctu.edu.tw)

‡Electronic address: [yyang@mail.nctu.edu.tw](mailto:yyang@mail.nctu.edu.tw)

## Contents

<b>I. Introduction</b>	2
<b>II. Einstein-Maxwell-Scalar System</b>	5
<b>III. Non-Backreaction</b>	9
<b>IV. Full-Backreaction</b>	14
A. Generalized Matching Solutions	15
B. Condensate	17
C. Conductivity	19
<b>V. Conclusion</b>	24
<b>Acknowledgements</b>	25
<b>Appendices</b>	25
<b>A. Condensate near critical temperature</b>	25
<b>B. Formulas with full-backreaction</b>	26
<b>References</b>	28

## I. INTRODUCTION

The superconductivity is an extraordinary important phenomena in condensed matter physics. It was first discovered by Onnes in 1911. In 1933, a famous property of the superconductors, the Meissner effect, had been observed. The symmetry breaking natural of the superconductor was then revealed by the phenomenological Ginzburg-Landau theory. In 1957, Bardeen, Cooper and Schrieffer proposed a microscopic theory which successfully describes the first type superconductivity, i.e. the BCS theory [1]. However, the materials in the real world have plenty properties beyond the BCS theory. The theoretical understanding of the strong-coupled superconductors still stayed in the barren land.

In the late 90's, Maldacena shed some light on the understanding of the notorious strong-coupled systems via the AdS/CFT conjecture, i.e. the holographic correspondence [2–6]. The holographic correspondence is a powerful tool to study a  $d + 1$ -dimensional strongly coupled conformal field theories (CFT) by studying its  $d + 2$ -dimensional dual gravitational theory in an Anti-de Sitter (AdS) space, and vice versa. There has been an upsurge to study the strong-coupled superconductors via the holographic correspondence since the pioneer work by Steven S. Gubser [7], and this kind of the superconductors models are usually called the holographic superconductors (HSC) [8–13].

HSC has been widely studied during the last decade by using various numerical methods [9, 12, 14–70] and analytic methods [71–87]. Many important properties of the strong-coupled superconductors have been successfully described by HSC. Nevertheless, the analytical grasp is still naive, far from the exact solutions due to the extremely complicated non-linear equations of motion of the dual gravity theory.

An approximated analytic method called matching method was proposed in [77] and has been used to study HSC recently [77–87]. In the matching method, the asymptotic expansions of the fields on the AdS boundary and the event horizon are matched at an intermediate point in the bulk. So far the matching method has only been applied in the non-backreaction case by treating the matter fields as probe fields.

In the non-backreaction case, the gravitational background is given and the probe matter fields are obtained by matching. Since the bulk behaviors and the gravity respendency of the fields in the bulk spacetime are sacrificed in the matching method, the matching solution is not the true solution of the equations of motion so that one might debate the validity of this method. However, the matching method does describe the critical behaviors of the HSC very well both qualitatively and quantitatively. We thus believe that the majority of the important physical properties of the holographic systems mainly depend on the asymptotic behaviors on the AdS boundary and the event horizon, but are not sensitive to the behaviors in the bulk at least in case of HSC.

Although the matching method applied in the non-backreaction case has successfully described the critical behaviors of HSC, the low temperature behavior is unsatisfactory. The condensation quickly becomes divergent when the temperature is cooled down from the critical value. This problem motivates us to study the HSC in the full backreaction case. In the full backreaction case, the gravitational background fields are obtained by matching as well

as the probe matter fields. Unfortunately, there is an obstruction which makes it inapplicable to extend the matching method to the full-backreaction case directly because the differential equations of motion for the background fields are first-order equations. Nevertheless, since the key point of the matching method should be matching of the boundary conditions on the conformal boundary of the AdS spacetime and the event horizon, we generalize the matching method to collect all the degrees of freedom on the boundaries by relaxing their smooth conditions for the background fields. The details will be shown in section IV.

In this work, we consider a non-minimal HSC model with two parameters that has been studied numerically in [16]. We study both the non-backreaction case using the ordinary matching method and the full-backreaction case using the generalized matching method. We calculate the scalar condensation and the critical temperature. The generalized matching method in the full-backreaction case produces the consistent results with the numerical ones in [16]. In addition, we study the electric conductivity using an analytic truncating method.

This paper is organized as follows: In section II, we introduce the EMS system and describe the matching method to solve the system. In section III, we study the condensate of dilaton in the non-backreaction case with the ordinary matching method. In section IV, we study the condensate with the generalized matching method and the electric conductivity in the full backreaction case. We summarize our results in section V.

(Unfortunately, there is a drawback of the matching method that the analytic description of the finite condensate region is still clueless. An additional approximation is required to have an analytic behavior of the condensate [81] at the temperature lower than the critical one. Nevertheless, we found that the low temperature behavior is dominated by the backreaction of the matter fields on the metric of the bulk spacetime. The  $\chi$  field which appears in the metric only in the backreaction case plays a crucial role.

Is there any possibility to remove the approximations? Our work is devoted to answer this question via generalizing the matching method and considering the full-backreaction.

There was an obstruction which makes the ordinary matching method inapplicable in the full-backreaction case. A naive interpretation lingers in one's mind that the continuous and smooth matching condition might be necessary but not enough, although they are not physical conditions. However, the main point of the matching method should be the matching of the boundary conditions on either the conformal boundary of the AdS spacetime or the event horizon in the bulk spacetime. The generalized matching method collects all

the boundary conditions by almost the same approach of the ordinary matching method.

The only difference between the generalized matching method and the ordinary one is relaxing the smooth matching condition for the matching of the gravity field. The details will be shown later.)

## II. EINSTEIN-MAXWELL-SCALAR SYSTEM

In this paper, we consider a 4-dimensional Einstein-Maxwell-Scalar (EMS) system, which includes a gravity field  $g_{\mu\nu}$ , a Maxwell field  $A_\mu$  and a charged complex scalar field  $\Phi = \phi e^{i\theta}$ . After fixing the Stückelberg field  $\theta = 0$ , the action can be expressed as,

$$S = \frac{1}{16\pi G_4} \int dz d^3x \sqrt{-g} \left[ R - \frac{f(\phi)}{4} F^{\mu\nu} F_{\mu\nu} + \frac{6}{\ell^2} U(\phi) - \frac{1}{2} (\partial^\mu \phi \partial_\mu \phi) - \frac{J(\phi)}{2} A^\mu A_\mu \right], \quad (2.1)$$

where  $f(\phi)$  is the gauge kinetic function which describes the interaction between the gauge field and the scalar field,  $U(\phi)$  is the scalar potential and  $J(\phi)$  is the extended Stückelberg function that preserve the gauge invariant. In this paper, we choose

$$f(\phi) = 1 + \frac{\alpha^2}{2} \phi^2, \quad (2.2a)$$

$$U(\phi) = 1 - \frac{\ell^2}{12} m^2 \phi^2, \quad (2.2b)$$

$$J(\phi) = q^2 \phi^2. \quad (2.2c)$$

The similar system has been studied numerically in [16]. There are four free parameters ( $\alpha, q, m, \ell$ ) in the action. We will analytically study the system by generalizing the matching method and compare our results with the ones in the numerical method.

The equations of motion are obtained by varying the action with the different fields,

$$R_{\mu\nu} - \frac{1}{2} g_{\mu\nu} \left[ R - \frac{f(\phi)}{4} F^{\rho\sigma} F_{\rho\sigma} + \frac{6}{\ell^2} U(\phi) - \frac{1}{2} (\partial^\rho \phi \partial_\rho \phi) - \frac{J(\phi)}{2} A^\rho A_\rho \right] - \frac{f(\phi)}{2} F_{\mu\rho} F_{\nu}{}^\rho - \frac{1}{2} \partial_\mu \phi \partial_\nu \phi - \frac{J(\phi)}{2} A_\mu A_\nu = 0, \quad (2.3a)$$

$$\nabla_\mu [f(\phi) F^{\mu\nu}] - J(\phi) A^\nu = 0, \quad (2.3b)$$

$$\nabla^2 \phi - \frac{1}{4} \frac{\partial f(\phi)}{\partial \phi} F^{\mu\nu} F_{\mu\nu} + \frac{6}{\ell^2} \frac{\partial U(\phi)}{\partial \phi} - \frac{1}{2} \frac{\partial J(\phi)}{\partial \phi} A^\mu A_\mu = 0. \quad (2.3c)$$

Since we are going to study the thermodynamic properties in the HSC system at the finite temperature, we consider a black hole background that asymptotic to the AdS space.

Without loss of generality, we consider the following ansatz of an isotropic black hole,

$$ds^2 = -g(r) e^{-\chi(r)} dt^2 + \frac{dr^2}{g(r)} + r^2 (dx^2 + dy^2), \quad (2.4a)$$

$$A = A_t(r) dt, \quad (2.4b)$$

$$\phi = \phi(r), \quad (2.4c)$$

where  $r$  is the holographic radius which corresponds to the energy scale in the dual field theory. The Hawking temperature of the black hole can be calculated as,

$$T = \frac{1}{4\pi} g(r)' e^{-\frac{\chi(r)}{2}} \Big|_{r=r_H}, \quad (2.5)$$

where the black hole horizon  $r_H$  is defined by  $g(r_H) = 0$ . Plugging the ansatz (2.4) into the equations of motion (2.3) leads to the following equations of motion for the background fields:

$$\chi' + \frac{r}{2} \phi'^2 + \frac{rJ}{2g^2} e^{\chi} A_t^2 = 0, \quad (2.6a)$$

$$\frac{g'}{rg} + \frac{1}{r^2} + \frac{1}{4} \phi'^2 - \frac{3}{\ell^2 g} U(\phi) + \frac{f}{4g} e^{\chi} A_t'^2 + \frac{J}{4g^2} e^{\chi} A_t^2 = 0, \quad (2.6b)$$

$$A_t'' + \left( \frac{f'}{f} + \frac{2}{r} + \frac{\chi'}{2} \right) A_t' - \frac{J}{gf} A_t = 0, \quad (2.6c)$$

$$\phi'' + \left( \frac{g'}{g} + \frac{2}{r} - \frac{\chi'}{2} \right) \phi' + \left( \frac{6U'}{\ell^2 g} + \frac{e^{\chi} A_t'^2 J f'}{2g} + \frac{e^{\chi} A_t^2 J'}{2g^2} \right) \frac{1}{\phi} = 0, \quad (2.6d)$$

where the prime represents the derivative with respect to  $r$ . It is easy to verify that the RN-AdS black hole is a simple solution of the above equations of motion (2.6),

$$g(r) = \frac{r^2}{\ell^2} - \frac{1}{r} \left( \frac{r_H^3}{\ell^2} + \frac{\rho^2}{4r_H} \right) + \frac{\rho^2}{4r^2}, \quad (2.7a)$$

$$A_t = \rho \left( \frac{1}{r_H} - \frac{1}{r} \right), \quad (2.7b)$$

$$\chi(r) = \phi(r) = 0. \quad (2.7c)$$

In this paper, we are going to find an approximate analytic solution of the equations of motion (2.6) using the matching method. Instead of solving the equations of motion (2.6) directly, we construct the asymptotic solutions first near both the horizon at  $r = r_H$  and the boundary at  $r = \infty$ , respectively. The solutions at the horizon and the boundary can be determined order by order given the appropriate boundary conditions. We then match the two asymptotic solutions at some intermediate points  $r_m \in (r_H, \infty)$  by requiring

the continuous and smooth conditions. However, there is an obstruction which makes it inapplicable to extend the matching method to the full-backreaction case directly because the differential equations of motion for the background fields are first-order equations. We solve the problem by relaxing the smooth matching conditions on the gravitational background fields. The details of the generalized matching method will be described in the section IV.

Obviously, the solutions by matching are only good approximations at the horizon and the boundary, but not the exact solutions of the equations of motion at every  $r$ . Nevertheless, since the core of the holographic correspondence is to relate the field theory on the boundary and the near horizon geometry of the bulk, we believe that the detail behavior of the solution at the intermediate part does not affect the physics too much. We thus can trust the physics from the results of this approximate matching solution at least qualitatively.

It is convenient to make a coordinate transformation from  $r$  to  $z = r_H/r \in (0, 1)$  with the boundary at  $z = 0$  and the black hole horizon at  $z = 1$ . In this work, to be concrete, we choose the matching point as  $z_m = 3/4$ . With the new coordinate  $z$ , the equations of motion for the background fields become,

$$\chi' - \frac{z}{2}\phi'^2 - \frac{r_H^2 B^2}{2z^3 g^2} = 0, \quad (2.8a)$$

$$g' - \left(\frac{1}{z} + \frac{\chi'}{2}\right)g - \frac{zf}{4}\left(B' - \frac{\chi'}{2}B\right)^2 + \frac{3r_H^2 U}{z^3 \ell^2} = 0, \quad (2.8b)$$

$$B'' + \left(\frac{f'}{f} - \frac{\chi'}{2}\right)B' - \left(\frac{\chi''}{2} + \frac{\chi' f'}{2f} + \frac{1}{z^4} \frac{r_H^2 J}{gf}\right)B = 0, \quad (2.8c)$$

$$\phi'' + \left(\frac{g'}{g} - \frac{\chi'}{2}\right)\phi' + \left[\frac{\left(B' - \frac{\chi'}{2}B\right)^2 f'}{2g} + \frac{r_H^2 B^2 J'}{2z^4 g^2} + \frac{6r_H^2 U'}{z^4 \ell^2 g}\right] \frac{1}{\phi'} = 0. \quad (2.8d)$$

where the prime represents the derivative with respect to  $z$  now, and we have defined a new field  $B^2 = e^{\chi} A_t^2$  for convenience.

The series expansions of the background fields near the horizon can be written as:

$$\chi(z) = \sum_{k=0}^{\infty} \chi_k (1-z)^k, \quad (2.9a)$$

$$g(z) = \frac{r_H^2}{\ell^2 z^2} \left[ 1 - z^3 + \sum_{k=0}^{\infty} g_k (1-z)^k \right], \quad (2.9b)$$

$$B(z) = \sum_{k=0}^{\infty} B_k (1-z)^k, \quad (2.9c)$$

$$\phi(z) = \sum_{k=0}^{\infty} \phi_k (1-z)^k, \quad (2.9d)$$

In the above expansions, because the differential equations for  $\chi$  and  $g$  are first order and the differential equations for  $B$  and  $\phi$  are second order, there are six coefficients  $(\chi_0, g_0, B_0, B_1, \phi_0, \phi_1)$  can be chosen as the boundary conditions at the horizon  $z = 1$ , while the other higher ordered coefficients can be obtained from these six coefficients by solving the equations of motion order by order.

Specially, the boundary condition to define the horizon  $g(1) = 0$  leads  $g_0 = 0$ . Furthermore, the regularity boundary conditions at the horizon require,

$$B_0 = 0, \quad (2.10a)$$

$$\phi_1 = -\frac{1}{g'} \left( 6 \frac{\partial U(\phi)}{\partial \phi} + \frac{B_1^2}{2} \frac{\partial f(\phi)}{\partial \phi} \right) \Big|_{z=1}. \quad (2.10b)$$

In this work, for the least approximation, we only take the expansions at the horizon up to the order  $k = 1$  for the fields  $\chi$  and  $g$ , and to the order  $k = 2$  for the fields  $B$  and  $\phi$ . The series expansion of the background fields near the horizon become,

$$\chi(z) = \chi_0 + \chi_1 (1-z), \quad (2.11a)$$

$$g(z) = \frac{r_H^2}{\ell^2 z^2} [1 - z^3 + g_1 (1-z)], \quad (2.11b)$$

$$B(z) = B_1 (1-z) + B_2 (1-z)^2, \quad (2.11c)$$

$$\phi(z) = \phi_0 + \phi_1 (1-z) + \phi_2 (1-z)^2, \quad (2.11d)$$

where  $\phi_1$  is given in Eq. (2.10b) and only three coefficients  $(\chi_0, B_1, \phi_0)$  left to be given.



At the boundary  $z = 0$ , the asymptotic behavior of the fields are,

$$\chi(z) \sim \chi^{(0)} + \frac{\Delta_{\pm}}{4\ell^2} \frac{D_{\Delta_{\pm}}^2}{r_H^{2\Delta_{\pm}}} z^{2\Delta_{\pm}}, \quad (2.12a)$$

$$g(z) \sim \begin{cases} \frac{r_H^2}{\ell^2 z^2} - \frac{2M}{r_H} z + \frac{\Delta_{\pm}}{4\ell^2} \frac{D_{\Delta_{\pm}}^2}{r_H^{2\Delta_{\pm}-2}} z^{2\Delta_{\pm}-2} & \frac{1}{2} < \Delta_{\pm} \leq \frac{3}{2}, \\ \frac{r_H^2}{\ell^2 z^2} - \frac{2M}{r_H} z & \frac{3}{2} < \Delta_{\pm}, \end{cases} \quad (2.12b)$$

$$B(z) \sim \mu - \frac{\rho}{r_H} z, \quad (2.12c)$$

$$\phi(z) \sim \frac{D_{\Delta_-}}{r_H^{\Delta_-}} z^{\Delta_-} + \frac{D_{\Delta_+}}{r_H^{\Delta_+}} z^{\Delta_+} \quad (2.12d)$$

where

$$\Delta_{\pm} = \frac{3 \pm \sqrt{9 + 4m^2\ell^2}}{2}. \quad (2.13)$$

are the conformal dimensions for the scalar fields with mass  $m$ .

Similarly, in the above asymptotic forms, there are six coefficients  $(\chi^{(0)}, M, \mu, \rho, D_{\Delta_-}, D_{\Delta_+})$  can be chosen as the boundary conditions at the boundary  $z = 0$ . The asymptotic coefficients  $\mu$  and  $\rho$  in  $B(z)$  are chemical potential and charge density. The asymptotic coefficients  $D_{\Delta_-}$  and  $D_{\Delta_+}$  in  $\phi(z)$  represent the condensates.

To satisfy the conformal symmetry, we should fix either  $D_{\Delta_-} = 0$  or  $D_{\Delta_+} = 0$  to obtain a stable solution. Both boundary conditions are allowed and we choose  $D_{\Delta_-} = 0$  for convention in this work. Setting  $m^2\ell^2 = -2$ , we have  $\Delta_- = 1$  and  $\Delta_+ = 2$ . With our choices, the asymptotic behavior of the background fields at the boundary  $z = 0$  becomes,

$$\chi(z)x \sim \chi^{(0)} + \frac{1}{2\ell^2} \frac{D_2^2}{r_H^4} z^4, \quad (2.14a)$$

$$g(z) \sim \frac{r_H^2}{\ell^2 z^2} - \frac{2M}{r_H} z, \quad (2.14b)$$

$$B(z) \sim \mu - \frac{\rho}{r_H} z, \quad (2.14c)$$

$$\phi(z) \sim \frac{D_2}{r_H^2} z^2, \quad (2.14d)$$

where only five coefficients  $(\chi^{(0)}, M, \mu, \rho, D_2)$  left to be given.

### III. NON-BACKREACTION

We first consider the case of non-backreaction, i.e. we treat the field  $\phi$  and  $B$  as the probe fields which do not affect the spacetime background. By setting  $\phi = B = 0$ , the equations

of motion (2.8) for the background fields reduces to

$$\chi' = 0, \quad (3.1a)$$

$$g' - \frac{g}{z} + \frac{3r_H^2}{z^3 \ell^2} = 0, \quad (3.1b)$$

which admits the simple AdS-Schwarzschild black hole solution,

$$\chi(z) = 0, \quad (3.2a)$$

$$g(z) = \frac{r_H^2}{\ell^2 z^2} (1 - z^3), \quad (3.2b)$$

with the black hole temperature  $T = 3r_H^2/\ell^2$ .

Next, we are going to solve the equations of motion for the probe fields  $B$  and  $\phi$ ,

$$B'' + \frac{f'(z)}{f} B' - \frac{1}{z^4} \frac{r_H^2 J}{g f} B = 0, \quad (3.3a)$$

$$\phi'' + \frac{g'}{g} \phi' + \left[ \frac{B'^2 f'}{2g} + \frac{r_H^2 B^2 J'}{2z^4 g^2} + \frac{6r_H^2 U'}{z^4 \ell^2 g} \right] \frac{1}{\phi'} = 0. \quad (3.3b)$$

There are two scaling symmetries in the equations of motion (3.3) with the form  $C \rightarrow s^{-n_C} C$ , where  $C$  is one of the variables  $(r, t, \vec{x}, g, B, \ell, q)$ ,  $s$  is a scaling factor and  $n_C$  is the scaling dimension for  $C$ . The scaling dimensions for the two scaling symmetries are listed in Table I.

Sym.	$n_r$	$n_t$	$n_{\vec{x}}$	$n_g$	$n_B$	$n_\ell$	$n_q$
I	1	-1	-1	2	1	0	0
II	1	0	1	0	0	1	-1

TABLE I: The two scaling symmetries of the equations of motion (3.3) in the case of non-backreaction.

We can use the above two scaling symmetries to set  $\ell = 1$  and  $\rho = \text{constant}$ . The generalized matching method is reduced to the ordinary matching method because there are only second order differential equations of motion.

In the case of non-backreaction, the series expansions of the fields  $B$  and  $\phi$  near the horizon in Eqs.(2.11) becomes,

$$B(z) = a(1-z) + B_2(1-z)^2, \quad (3.4a)$$

$$\phi(z) = b + \phi_1(1-z) + \phi_2(1-z)^2, \quad (3.4b)$$

where we have renamed  $B_1 = a$  and  $\phi_0 = b$  in (2.11).  $a$  and  $b$  will be imposed as the boundary values at the horizon  $z = 1$ . Plug the series expansions (3.4) into the equations of motion (3.3),  $B_2$ ,  $\phi_1$  and  $\phi_2$  can be solved in terms of the boundary values  $a$  and  $b$  order by order,

$$B_2 = \frac{1}{6} \frac{((4\alpha^2 + 2q^2)r_H^2 + a^2\alpha^4)b^2a}{r_H^2(\alpha^2b^2 + 2)}, \quad (3.5a)$$

$$\phi_1 = -\frac{1}{6} \frac{b(\alpha^2a^2 + 4r_H^2)}{r_H^2} \quad (3.5b)$$

$$\begin{aligned} \phi_2 = & -\frac{1}{48} \frac{b}{r_H^4(\alpha^2b^2 + 2)} \left\{ \left( \frac{32\alpha^2b^2}{3} + \frac{64}{3} \right) r_H^4 \right. \\ & \left. + 4a^2 \left[ -\frac{1}{3}\alpha^4b^2 + \left( b^2q^2 - \frac{10}{3} \right) \alpha^2 + \frac{2}{3}q^2 \right] r_H^2 + a^4\alpha^4 \left( \alpha^2b^2 - \frac{2}{3} \right) \right\}. \end{aligned} \quad (3.5c)$$

At the boundary  $z = 0$ , the asymptotic behavior of the fields  $B$  and  $\phi$  are the same as in Eqs. (2.14),

$$B(z) \sim \mu - \frac{\rho}{r_H} z, \quad (3.6a)$$

$$\phi(z) \sim \frac{D_2}{r_H^2} z^2. \quad (3.6b)$$

where  $\mu$  and  $D_2$  will be imposed as the boundary values at the boundary  $z = 0$ .

The two boundary values  $a$  and  $b$  at the horizon  $z = 1$  and the two boundary values  $\mu$  and  $D_2$  at the boundary  $z = 0$  are related by the matching conditions of the fields  $B$  and  $\phi$  at a matching point  $z_m$ .

To match the series expansions of the fields  $B(z)$  and  $\phi(z)$  at the horizon in Eq. (3.4) and that at the boundary in Eq. (3.6) smoothly at a matching point  $z_m$ , we require the following four constraint equations,

$$\mu - \frac{\rho}{r_H} z_m = a(1 - z_B) + B_2(1 - z_m)^2, \quad (3.7a)$$

$$-\frac{\rho}{r_H} = -a - 2B_2(1 - z_B), \quad (3.7b)$$

$$\frac{D_2}{r_H^2} z_m^2 = b + \phi_1(1 - z_m) + \phi_2(1 - z_m)^2, \quad (3.7c)$$

$$\frac{2D_2}{r_H^2} z_m = -\phi_1 - 2\phi_2(1 - z_m). \quad (3.7d)$$

The above constraint equations can be solved as,

$$\mu = a + B_2 (1 - z_m) (1 + z_m), \quad (3.8a)$$

$$\rho = [a + 2B_2 (1 - z_m)] r_H, \quad (3.8b)$$

$$D_2 = \frac{b}{12z_m} [12r_H^2 - (\alpha^2 a^2 + 4r_H^2)(1 - z_m)], \quad (3.8c)$$

$$0 = 2b + \phi_1 (2 - z_m) + 2\phi_2 (1 - z_m), \quad (3.8d)$$

To be concrete, we take  $z_m = 3/4$  in the following calculation. The two parameters  $a$  and  $b$  can be analytically solved from Eqs. (3.8b) and (3.8d) once the charge density  $\rho$  is given,

$$b^2 = \frac{-24r_H(ar_H - \rho)}{2a(8\alpha^2 + q^2)r_H^2 - 12\alpha^2 r_H \rho + \alpha^4 a^3}, \quad (3.9)$$

with  $a$  satisfies a quartic equation,

$$\alpha^4 a^4 - 4r_H^2(-2\alpha^2 + q^2)a^2 - 48r_H \rho \alpha^2 a + 304r_H^4 = 0. \quad (3.10)$$

The condensate  $D_2$  is the order parameter of the superconducting phase transition. Above a critical temperature  $T_c$ , the order parameter  $D_2 \propto b$  is zero, which from Eq. (3.9) implies  $ar_H - \rho = 0$  at the critical temperature  $T_c$ . From Eq. (3.10), we obtain the critical temperature by taking  $a = \rho/r_H$ ,

$$T_c = \frac{3}{4\pi} \left( \frac{10\alpha^2 + q^2 + \sqrt{24\alpha^4 + 20\alpha^2 q^2 + q^4}}{152} \right)^{1/4} \rho^{1/2}. \quad (3.11)$$

For  $\alpha = q = 0$ ,  $T_c$  vanishes, there is no phase transition at this special point. For  $\alpha \gg q$ , the critical temperature  $T_c \propto \alpha^{1/2}$ ; While for  $\alpha \ll q$ , the critical temperature  $T_c \propto q^{1/2}$ . The critical temperature  $T_c$  is proportional to  $\sqrt{\rho}$  and increases with  $\alpha$  and  $q$  monotonously.  $T_c/\sqrt{\rho}$  vs. the parameters  $(\alpha, q)$  is plotted in Fig. 1. The behavior of the analytic expression of the critical temperature in Eq. (3.11) is consistent with the numeric result in [16].

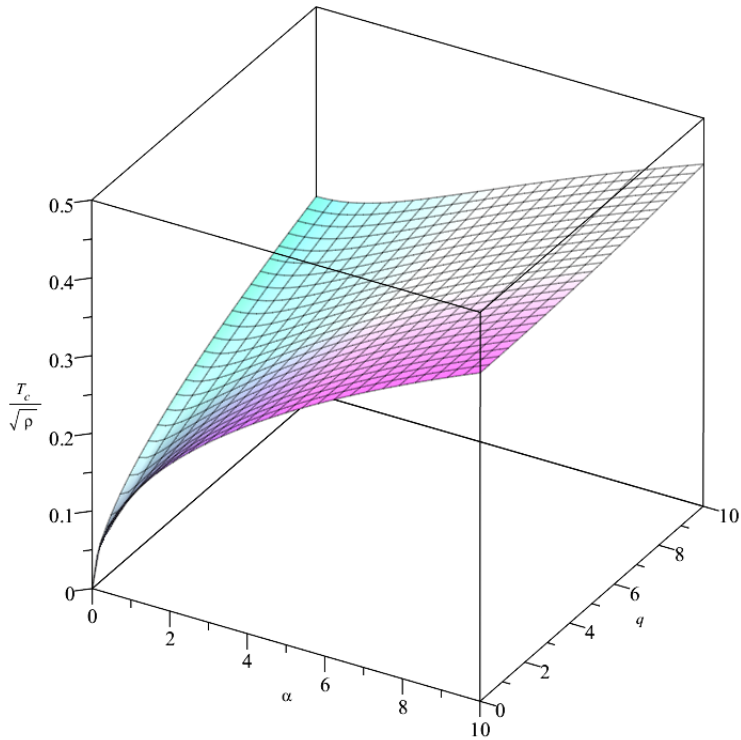


FIG. 1:  $T_c/\sqrt{\rho}$  varies with the couplings  $\alpha, q$ .

Near the critical temperature  $T_c$ , the condensate behaves as  $D_2 = AT_c^2(1 - T/T_c)^{1/2}$ , which indicates that the phase transition at  $T_c$  is a second order phase transition. The coefficient  $A$  depends on the parameters  $\alpha, q$  and  $\rho$ , see Eq. (A.1) in the Appendix.

The condensate  $D_2$  vs.  $T/T_c$  for  $\alpha = q = 1$  can be calculated from Eq. (3.8c) and is plotted as the solid line in Fig. 2. We see that the low temperature behavior of condensate in the non-backreaction calculation (red line) is not consistent with the numeric calculation in [16]. The blue line in Fig. 2 is the condensate near the critical temperature and is exploited to the low temperature region. The Fig. 2 shows the drawback of the non-backreaction approximation that is also seen in [81]. This drawback seeks an improvement on the ordinary matching method.

The inconsistency of the condensate around the low temperature is due to the non-backreaction approximation we took in this section. In the next section, we will study the full backreaction case.

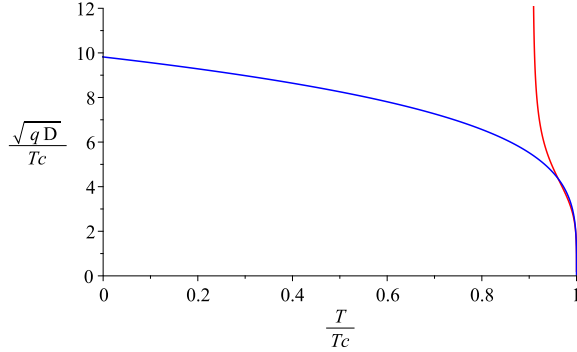


FIG. 2: The behavior of the condensate  $D_2$  with the couplings  $\alpha = 1$ ,  $q = 1$ . The red line is the condensate directly from Eq. (3.8c), while the blue line is the approximate condensate near the critical temperature  $T_c$ .

#### IV. FULL-BACKREACTION

In this section, we consider the case of full-backreaction by including the backreacted effects of the fields  $B$  and  $\phi$ . It is necessary to solve the fields  $\chi$  and  $g$  in the metric (2.4a) as well as the fields  $B$  and  $\phi$  together from the full equations of motion (2.8).

Similarly to the non-backreaction case, there are three scaling symmetries in the equations of motion (2.8) in the full-backreaction case. The scaling dimensions of these variables for the scaling symmetries are listed in Table II.

Sym.	$n_r$	$n_t$	$n_{\vec{x}}$	$n_{r_H}$	$n_{e\chi}$	$n_g$	$n_B$	$n_\ell$	$n_q$
I	1	1	0	0	2	0	0	0	0
II	1	-1	-1	1	0	2	1	0	0
III	1	1	0	1	0	0	0	1	-1

TABLE II: Scaling symmetries in the equations of motion (2.8) with full-backreaction.

As in the non-backreaction case, we can use the three scaling symmetries to set the parameters  $\ell = 1$ ,  $\rho = \text{constant}$  and  $\chi^{(0)} = 0$  in Eq. (2.12a), which are the necessary boundary conditions to ensure the asymptotic AdS at the boundary.

## A. Generalized Matching Solutions

Similarly as what we have done in the non-backreaction case, we will solve the fields  $(\chi, g, B, \phi)$  in the full-backreaction case by using the matching method.

Up to the order next to the initial values, the series expansions of the fields  $(\chi, g, B, \phi)$  near horizon in (2.11) becomes,

$$\chi(z) = \chi_0 + \chi_1(1-z), \quad (4.1a)$$

$$g(z) = \frac{r_H^2}{z^2} [1 - z^3 + g_1(1-z)], \quad (4.1b)$$

$$B(z) = a(1-z) + B_2(1-z)^2, \quad (4.1c)$$

$$\phi(z) = b + \phi_1(1-z) + \phi_2(1-z)^2, \quad (4.1d)$$

where we have renamed  $B_1 = a$  and  $\phi_0 = b$  in (2.11). In the above expansion,  $\chi_0$ ,  $a$  and  $b$  need to be imposed as the boundary values at the horizon  $z = 1$ . Plug the series expansions (4.1) into the equations of motion (2.8), we can solve for the coefficients  $(\chi_1, g_1, B_2, \phi_2)$  in Eqs. (4.1) in terms of the boundary values  $(\chi_0, a, b)$ .

$$g_1 = \frac{1}{8r_H^2} \left( 4b^2 r_H^2 - a^2(\alpha^2 b^2 + 2) \right), \quad (4.2a)$$

$$\phi_1 = -\frac{(a^2 \alpha^2 + 4r_H^2)b}{2(g_1 + 3)r_H^2}, \quad (4.2b)$$

$$\chi_1 = \frac{-\phi_1^2(g_1 + 3)^2 r_H^2 - a^2}{2(g_1 + 3)^2 r_H^2}, \quad (4.2c)$$

$$B_2 = \frac{a \left[ \left( \frac{1}{4} \chi_1 (g_1 + 3) \alpha^2 + q^2 \right) b^2 - \phi_1 \alpha^2 (g_1 + 3) b + \frac{1}{2} (g_1 + 3) \chi_1 \right]}{(\alpha^2 b^2 + 2)(g_1 + 3)}, \quad (4.2d)$$

$$\begin{aligned} \phi_2 = \frac{1}{8(g_1 + 3)^2 r_H^2} \left\{ \left[ \left( (\chi_1 + 4)b - \phi_1 \right) g_1 + (3\chi_1 + 15)b - 3\phi_1 \right] \alpha^2 - 2bq^2 \right] a^2 - 4bB_2 \alpha^2 (g_1 + 3)a \\ + 12r_H^2 \left[ \frac{1}{12} g_1^2 \chi_1 \phi_1 + \frac{1}{2} \left( \chi_1 + \frac{7}{3} \right) \phi_1 g_1 + b + \phi_1 \left( \frac{3}{4} \chi_1 + \frac{7}{2} \right) \right] \right\}. \end{aligned} \quad (4.2e)$$

The detailed forms are listed in (B.2).

At the boundary  $z = 0$ , the asymptotic behavior of the fields  $(\chi, g, B, \phi)$  was listed in Eq. (2.14), where  $M$ ,  $\mu$  and  $D_2$  will be imposed as the boundary values at the boundary  $z = 0$ .

The three boundary values  $(\chi_0, a, b)$  at the horizon  $z = 1$  and the three boundary values  $(M, \mu, D_2)$  at the boundary  $z = 0$  are related by six matching conditions of the fields  $(\chi, g, B, \phi)$  at a matching point  $z_m$ .

We match the asymptotic forms of the fields at the horizon in Eq. (2.14) and that at the boundary in Eq. (4.1) at a matching point  $z_m$ . Besides the four matching equations (3.7a -3.7d) for the matter fields as we listed in the non-backreaction case, additional matching constraints are needed for the gravitational fields. The equations of motion for the gravitational fields  $\chi(z)$  and  $g(z)$  are first order differential equations as shown in Eq. (2.8a) and Eq.(2.8c), so that we can only assign two boundary conditions. Therefore, only two more continuous matching conditions are applied on the gravitational fields

$$\frac{1}{2} \left( \frac{D_2 z_m^2}{r_H^2} \right)^2 = \chi_0 + \chi_1 (1 - z_m), \quad (4.3a)$$

$$\frac{1 - 2M z_m^3 r_H^2}{z_m^2} = \frac{1 - z_m^3}{z_m^2} r_H^2 + g_1 \frac{(1 - z_m)}{z_m^2} r_H^2, \quad (4.3b)$$

and we have to give up the smooth conditions.

The total six matching equations (3.7a -3.7d) and (4.3a -4.3b) can be solved as

$$\chi_0 = -\chi_1 (1 - z_m) + \frac{1}{2} \left( \frac{D_2}{r_H^2} \right)^2 z_m^4, \quad (4.4a)$$

$$M = \frac{1}{2} - \frac{g_1 (1 - z_m)}{2z_m^3}, \quad (4.4b)$$

$$\mu = a + B_2 (1 - z_m) (1 + z_m), \quad (4.4c)$$

$$\rho = \left[ a + 2B_2 (1 - z_m) \right] r_H, \quad (4.4d)$$

$$D_2 = \frac{2b + \phi_1 (1 - z_m)}{2z_m} r_H^2, \quad (4.4e)$$

$$0 = 2b + \phi_1 (2 - z_m) + 2\phi_2 (1 - z_m). \quad (4.4f)$$

The same as in the non-backreaction case, we take  $z_m = 3/4$  in the following. Eq.(4.4f) can be expressed as a cubic equation of  $a^2$ , see Eq. (B.6), which can be solved analytically in term of  $b^2$ .

We check the stability of the analytic hairy black hole solution by comparing its free energies with the free energies of RN black holes are obtained in Eqs. (2.7),

$$F_{\text{Hairy}} = V (-2M + \mu\rho), \quad (4.5a)$$

$$F_{\text{RN}} = \frac{V}{r_H} \left( -r_H^4 + \frac{3\rho^2}{4} \right). \quad (4.5b)$$

For the given couplings  $\alpha$  and  $q$ , as well as a charge density  $\rho$ , the free energies  $F_{\text{Hairy}}$  and  $F_{\text{RN}}$  vs.  $T/T_c$  are plotted in Fig. 3.



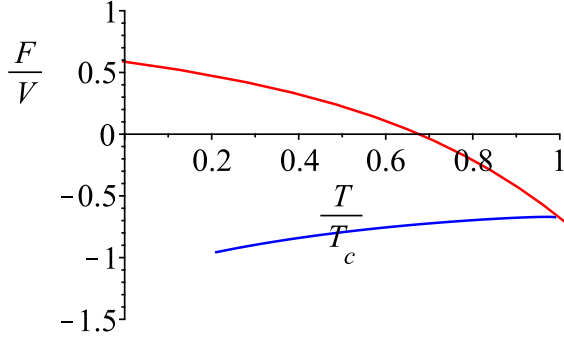


FIG. 3: The free energies  $\frac{F_{\text{Hairy}}}{V}$  (blue) and  $\frac{F_{\text{RN}}}{V}$  (red) with  $\alpha = 5$ ,  $q = 1$ , and  $\rho = \text{constant}$  for  $T \leq T_c$ .

When  $T < T_c$ , the free energy of the hairy black hole is always lower than that of the RN black hole and vice versa. Thus for  $T > T_c$ , the system is in the RN black hole phase with the scalar field  $\phi = 0$ ; while for  $T < T_c$ , the system transits to the hairy black hole phase with  $\phi \neq 0$  that indicates the condensation.

## B. Condensate

In this section, we investigate the condensate  $D_2$ , the order parameter of the superconducting phase transition, in more details. The behavior of the order parameter  $D_2 \propto b$  around the critical temperature is the same as that in the non-backreaction case,  $D_2 \propto (1 - T/T_c)^{1/2}$ . However, the fixed- $\rho$  condition has been modified at the critical temperature ( $B_2|_{T=T_c} \neq 0$ ). The condensate  $D_2$  vs the ratio of the temperature  $T/T_c$  for different parameters  $\alpha$  and  $q$  are plotted in Fig. 4 and 5.

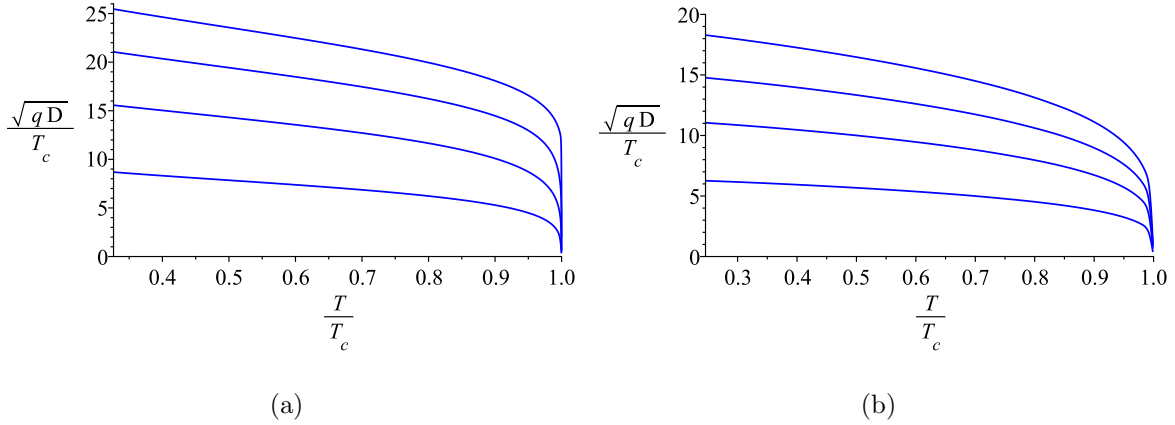


FIG. 4: The condensate to temperature diagram with the coupling  $q = 1, 3, 5, 7$  from bottom to top and (a)  $\alpha = 1$ , (b)  $\alpha = 5$ .

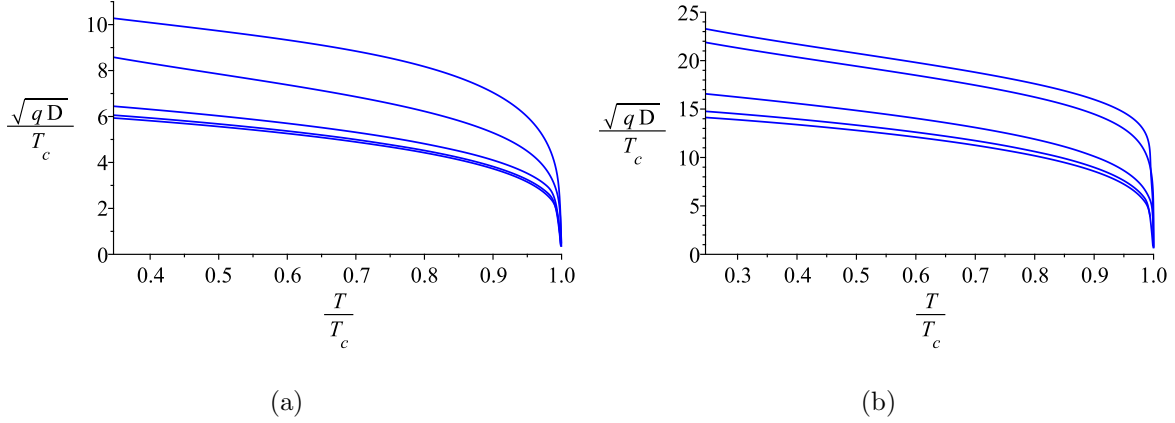


FIG. 5: The condensate to temperature diagram with the coupling  $\alpha = 10^{-4}, 1, 3, 5, 7$  from top to bottom and (a)  $q = 1$ , (b)  $q = 5$ .

From Fig. 4 and Fig. condensate alpha, we see that, for a fixed  $\alpha$ , the condensate  $D_2$  increases as the parameter  $q$  increases, while for a fixed  $q$ , the condensate  $D_2$  decreases as the parameter  $\alpha$  increases. The behavior of the condensate  $D_2$  depending on the parameters  $\alpha$  and  $q$  is consistent with the numeric result in [16].

As we did in the non-backreaction case, the critical temperature in the full-backreaction case can be obtained analytically, but the expression is much more complicated. The behavior of the critical temperature  $T_c$  in the full-backreaction case is also similar to that in the non-backreaction case and is plotted in Fig. 6.

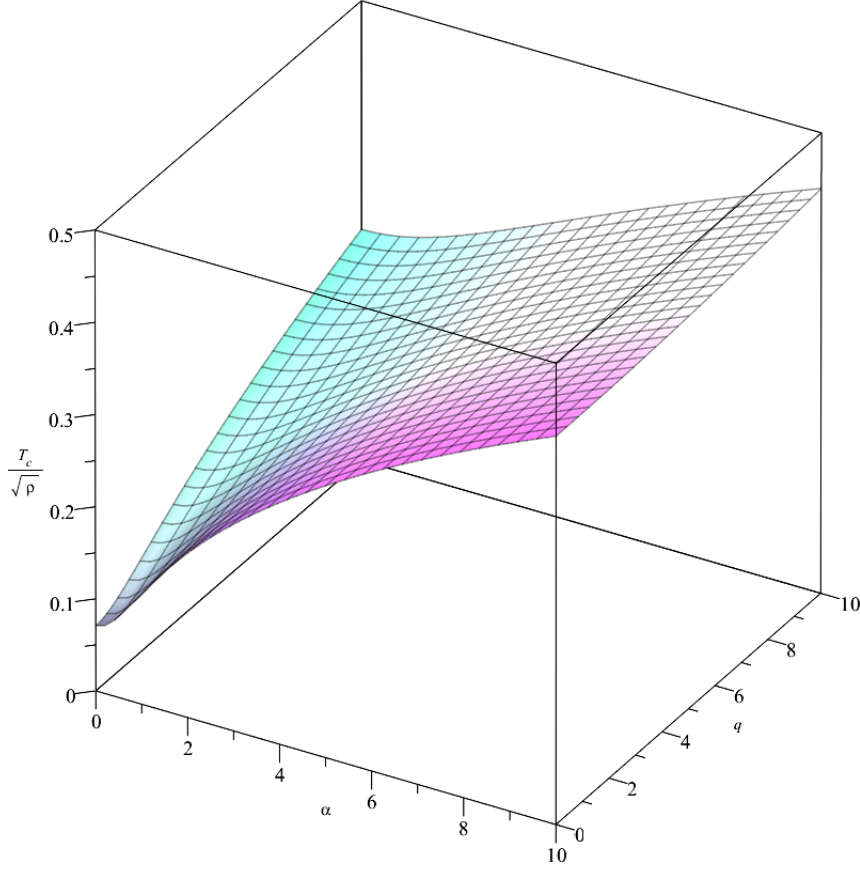


FIG. 6: The critical temperature  $T_c$  vary with the couplings  $\alpha$ ,  $q$ .

### C. Conductivity

In this section, we compute the conductivity of this system by adding an external source  $A_x$  perturbatively. The metric is thus modified by a perturbative non-diagonal component  $g_{tx}$ . Defining  $A_x = \tilde{A}_x(r) e^{-i\omega t}$  and  $g_{tx} = \tilde{g}_{tx}(r) e^{-i\omega t}$ , the equations of motion for the perturbative field  $\tilde{A}_x(r)$  and  $\tilde{g}_{tx}(r)$  are

$$\tilde{A}_x'' + \left( \frac{g'}{g} - \frac{\chi'}{2} + \frac{f'}{f} \right) \tilde{A}_x' + \left( \frac{\omega^2}{g^2} e^\chi - \frac{J}{gf} \right) \tilde{A}_x + \frac{A_t'}{g} e^\chi \left( \tilde{g}'_{tx} - \frac{2}{r} \tilde{g}_{tx} \right) = 0, \quad (4.6a)$$

$$\tilde{g}'_{tx} - \frac{2}{r} \tilde{g}_{tx} + f A_t' \tilde{A}_x = 0, \quad (4.6b)$$

which lead to a homogeneous linear differential equation for  $\tilde{A}_x$ ,

$$\tilde{A}_x'' + \left( \frac{g'}{g} - \frac{\chi'}{2} + \frac{f'}{f} \right) \tilde{A}_x' + \left[ \left( \frac{\omega^2}{g^2} - \frac{f A_t'^2}{g} \right) e^\chi - \frac{J}{gf} \right] \tilde{A}_x = 0. \quad (4.7)$$

Making a coordinate transformation  $z = r_H/r$  and defining  $e^\chi \tilde{A}_x^2 = C^2$ , the equation for  $\tilde{A}_x$  becomes

$$C''' + \left( \frac{g'}{g} - \frac{3}{2}\chi' + \frac{f'}{f} + \frac{2}{z} \right) C'' + \left[ -\frac{1}{2}\chi'' + \frac{1}{2}\chi'^2 - \frac{1}{2}\chi' \left( \frac{g'}{g} + \frac{f'}{f} + \frac{2}{z} \right) + \left( \frac{r_H^2 \omega^2 e^\chi}{z^4 g^2} - \frac{f}{g} \left( B' - \frac{1}{2}\chi' B \right)^2 - \frac{r_H^2 J}{z^4 g f} \right) \right] C = 0. \quad (4.8)$$

To realize the structure of the Eq. (4.8), we make a further coordinate transformation,

$$du = -\frac{r_H e^{\frac{\chi}{2}}}{g z^2} dz, \quad (4.9)$$

which transforms the horizon at  $z = 1$  to  $u = -\infty$  and the boundary at  $z = 0$  to  $u = 0$ .

We integrate the coordinate transformation (4.9) term by term to get

$$u = -\int \left( \frac{p_0}{1-z} + p_1 + \dots \right) dz = p_0 \ln(1-z) + p_1(1-z) + \dots, \quad (4.10)$$

where  $p_i$ 's are the expansion coefficients near the horizon at  $z = 1$ .

By defining a new field  $\Psi = \sqrt{f} e^{-\chi/2} C$ , the Eq.(4.8) can be brought to the form of the Schrodinger equation,

$$\frac{d^2 \Psi}{du^2} + [\omega^2 - V(u)] \Psi = 0, \quad (4.11)$$

where the potential is

$$V(u) = g \left[ f \left( \frac{d(e^{-\chi/2} B)}{du} \right)^2 + \frac{J}{f} e^{-\chi} \right] + \frac{1}{\sqrt{f}} \frac{d^2 \sqrt{f}}{du^2}, \quad (4.12)$$

with  $V(0) = V(-\infty) = 0$ .

The Schrodinger equation (4.11) with the potential (4.12) is a standard one-dimensional scattering problem, and the wave function  $\Psi(u)$  near the boundary at  $u \sim 0$  behaves as

$$\Psi(u) = e^{-i\omega u} + R e^{i\omega u}, \quad (4.13)$$

where  $R$  is the reflection coefficient. The conductivity can thus be written as

$$\sigma(\omega) = \frac{1-R}{1+R}. \quad (4.14)$$

At the horizon at  $u = -\infty$ , the in-falling wave boundary condition admits a non-reflection wave function ,

$$\Psi(u) = T e^{-i\omega u}. \quad (4.15)$$

where  $T$  is the transmission coefficient.

In the  $z$  coordinate, the in-falling wave function becomes

$$\Psi = T e^{-i\omega[p_0 \ln(1-z) + p_1(1-z) + \dots]}. \quad (4.16)$$

Therefore, near the horizon, the field  $C(z)$  can be expanded as,

$$\begin{aligned} C(z) &= c_0 e^{-i\omega[p_0 \ln(1-z) + p_1(1-z) + \dots]} \cdot [1 + C_1(1-z) + \dots] \\ &\simeq c_0 e^{-i\omega[p_0 \ln(1-z) + P_1(1-z)]} \cdot [1 + C_1(1-z)], \end{aligned} \quad (4.17)$$

where in the second line we assumed a truncated form of the field  $C(z)$  with  $P_1$  and  $C_1$  being the effective coefficients by truncating all the higher-order terms at the horizon. Therefore,  $P_1$  and  $C_1$  contain the effects far from the horizon and will be determined by Eq. (4.17) and the boundary condition at  $z = 0$ . The truncating solution is an approximation of the true solution, but we will see that many important properties are preserved in this approximation.

At the boundary, the asymptotic form of  $C(z)$  is

$$C(z) = C^{(0)} + \frac{C^{(1)}}{r_H} z + \dots. \quad (4.18)$$

Expanding the field  $C(z)$  in Eq. (4.17) at the boundary  $z = 0$ , the conductivity can be calculated as follows [9],

$$\sigma(\omega) = \frac{1}{i\omega} \frac{C^{(1)}}{C^{(0)}} = r_H(p_0 + P_1) - \frac{r_H}{i\omega} \left( \frac{C_1}{1 + C_1} \right). \quad (4.19)$$

In the high frequency limit  $\omega \rightarrow \infty$ , the conductivity should approach to one due to the asymptotic AdS geometry, the above expression gives

$$P_1 = -p_0 + \frac{1}{r_H}. \quad (4.20)$$

The coefficients  $p_0$  and  $C_1$  can be now calculated by plugging the the field  $C(z)$  in Eq. (4.17) into the equation of motion (4.8). The exact expressions of  $p_0$  and  $C_1$  are listed in the Appendix as Eqs. (B.3a) and (B.3b)..

The DC conductivity can be obtained from the low frequency expansion of the conductivity (4.19),

$$\sigma(\omega) = \Re(\sigma) + i\Im(\sigma), \quad (4.21)$$

$$\Re(\sigma) = \sigma_0 + O(\omega^2), \quad (4.22)$$

$$\Im(\sigma) = \sigma_{-1}\omega^{-1} + O(\omega). \quad (4.23)$$

where both  $\sigma_0$  and  $\sigma_{-1}$  are real and they are given in Eq. (B.7) in the Appendix. At  $\omega = 0$ , the imaginary part of the conductivity  $\Im(\sigma)$  is proportional to  $\omega^{-1}$ . By Kramers-Kronig relations, this implies that the real part of the conductivity  $\Re(\sigma)$  behaves as a delta function at  $\omega = 0$ , i.e. DC superconductivity.

In the high frequency, the conductivity can be expanded as,

$$\sigma(\omega) = 1 + \frac{i r_H}{\omega} + O(\omega^{-2}), \quad (4.24)$$

which gives  $\sigma(\omega) \rightarrow 1$  as  $\omega \rightarrow \infty$  that has been fixed by the choice of  $P_1$  in Eq. (4.20).

The real and imaginary parts of the conductivity vs. frequency are plotted in Fig. 7 - 9.

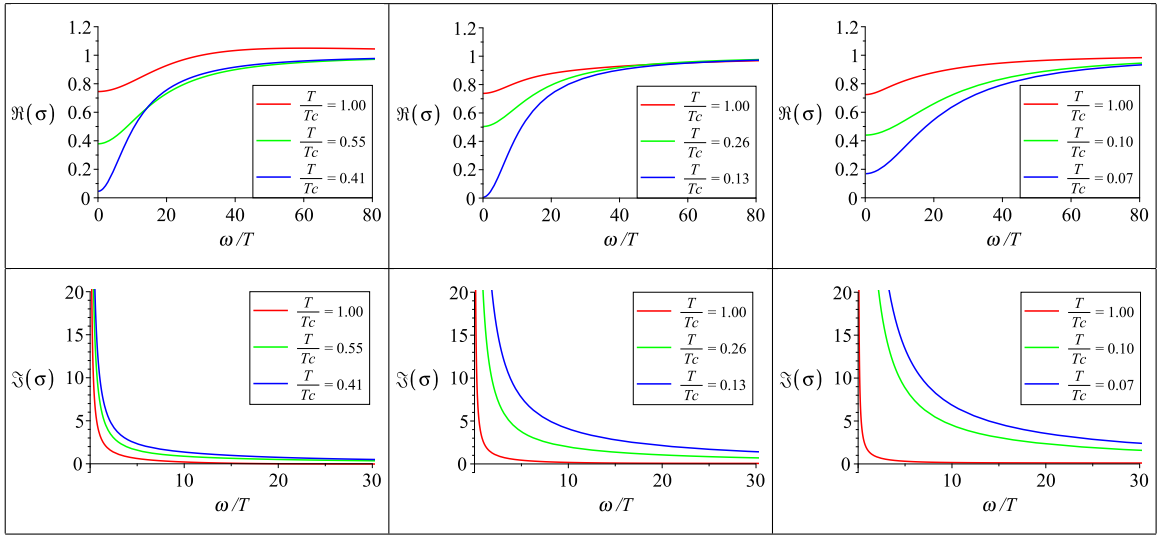


FIG. 7: The real and imaginary part of the conductivity with  $\alpha = 1$  and  $q = 1, 3, 5$  from left to right. The different curves in each figure are respect to different temperature ratio.

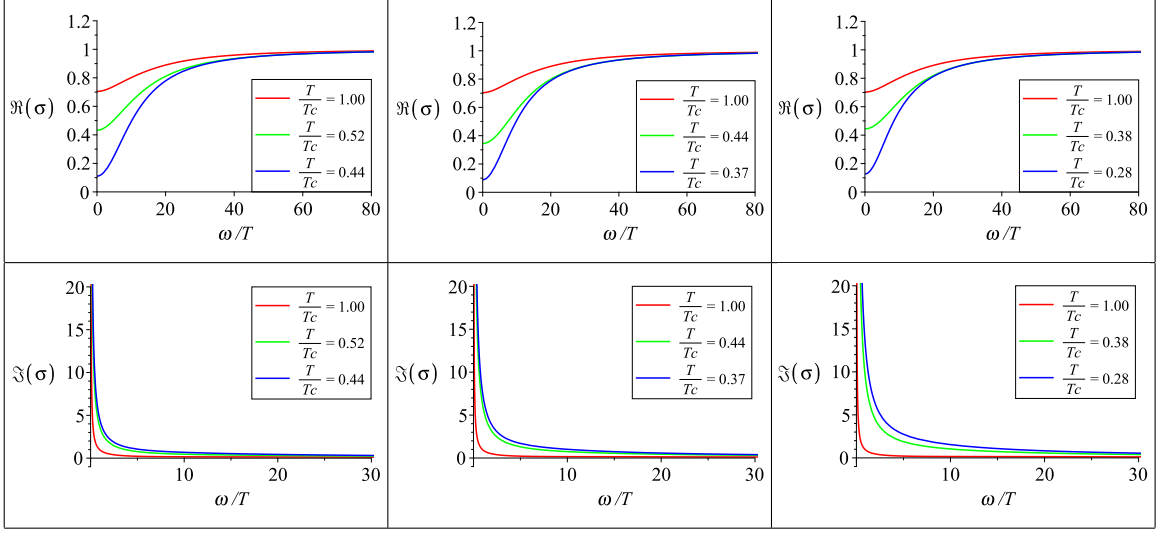


FIG. 8: The real and imaginary part of the conductivity with  $\alpha = 3$  and  $q = 1, 3, 5$  from left to right. The different curves in each figure are respect to different temperature ratio.

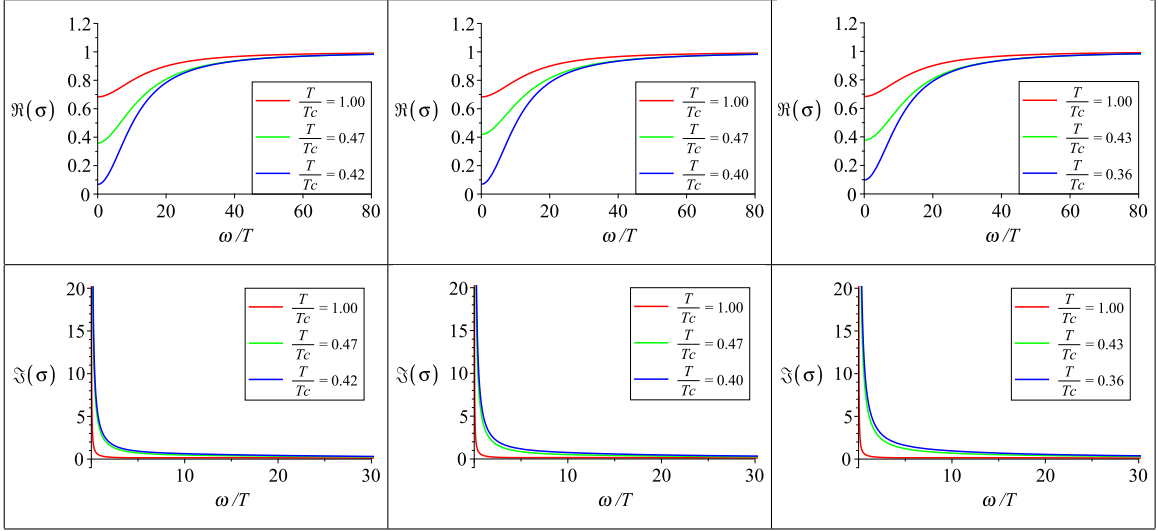


FIG. 9: The real and imaginary part of the conductivity with  $\alpha = 5$  and  $q = 1, 3, 5$  from left to right. The different curves in each figure are respect to different temperature ratio.

## V. CONCLUSION

We have seen that the generalized matching method can be regarded as collecting the boundary conditions which are located at several positions. The well behaved fields can have a series expansion while all the degrees of freedom for the initial values are determined via the boundary conditions at the point of the series expansion. It is not surprising that the simple boundary-conditions-collecting approach does work because of the achievement of the ordinary matching method.

In this paper, we studied a non-minimal HSC model by considering the Einstein-Maxwell-Dilaton system with both the non-backreaction and the full-backreaction cases by the matching method. The model has two adjustable parameters  $\alpha$  and  $q$ .  $\alpha$  describes the coupling between the Maxwell field and the dilaton, and  $q$  represents the charge of the dilaton.

We found that the critical temperature  $T_c$  of the phase transition does not depend on the backreaction of the gravitational background. The critical temperature increases with  $\alpha$  and  $q$  monotonously and behaves as  $T_c \propto \alpha^{1/2}$  for small  $q$  and  $T_c \propto q^{1/2}$  for small  $\alpha$ , which is consistent with the numeric results. The condensate near the critical temperature behaves as  $(1 - T/T_c)^{1/2}$  which indicates that the phase transition is second order.

We showed that, in the non-backreaction case, the behavior of the condensate at low temperature blows up quickly and is not make sense, while in the full-backreaction case, the low temperature behavior of the condensate is rectified. For a fixed  $\alpha$ , the condensate increases as the parameter  $q$  increases, while for a fixed  $q$ , the condensate decreases as the parameter  $\alpha$  increases. The behavior of the condensate depending on the parameters  $\alpha$  and  $q$  is consistent with the numeric result.

In addition, we developed an approximate analytic method to calculate the electric conductivity. We expand the perturbative field  $A_x$  near the horizon obliged on the in-falling boundary condition of the Schrodinger equation at the horizon. We then truncated the expansion to the linear order and determined the truncating coefficients by the equation of motion and the boundary condition at the boundary. We analytically showed that the imaginary part of the conductivity suffers a  $1/\omega$  divergence at small frequency that implies the Dirac  $\delta$  function behavior in the real part of the conductivity, i.e. DC superconductivity. Furthermore, we showed that the asymptotic values of the real conductivity in the small frequency limit increases as the temperature raised. However, we did not observe the "Drude



Peak” behavior at the low frequency as in the numeric calculation [16].

The matching method provides an analytic description of the HSC model. It help us to understand the analytic behaviors of the superconductors comparing to the numeric study. We believe that the analytic method could reveal more and more important properties of superconductors in the future.

### Acknowledgements

We thank Chiang-Mei Chen, Mei Huang, Ming-Fan Wu and Pei-Hung Yuan for useful discussion. This work is supported by the Ministry of Science and Technology (MOST 106-2112-M-009-005-MY3) and in part by National Center for Theoretical Science (NCTS), Taiwan.

# Appendices

## A. CONDENSATE NEAR CRITICAL TEMPERATURE

Expanding the condensate around the critical temperature  $T_c$ , we obtain the approximate condensate for  $T \leq T_c$ ,

$$D_2 = AT_c^2 \left( -\frac{T - T_c}{T_c} \right)^{1/2}, \quad (\text{A.1a})$$

$$A = \frac{11264\pi^4 T_c^4 - 81\alpha^2 \rho^2}{5184\pi^2 T_c^4} \left( -\frac{T_c}{T_1} \right)^{1/2}, \quad (\text{A.1b})$$

$$T = T_c + T_1 b^2 + O(b^4), \quad (\text{A.1c})$$

$$T_1 = \frac{\pi^4 \left( -2125824\pi^4 T_c^4 \alpha^2 - 77824\pi^4 T_c^4 q^2 + 22356\alpha^4 \rho^2 + 5670\alpha^2 q^2 \rho^2 + 243q^4 \rho^2 \right) T_c^5}{1944\rho^2 \left( \pi^4 T_c^4 q^2 + 10\pi^4 T_c^4 \alpha^2 - \frac{81\alpha^4 \rho^2}{512} \right)}, \quad (\text{A.1d})$$

## B. FORMULAS WITH FULL-BACKREACTION

The near horizon coefficients with full-backreaction are listed here. The coefficients for the condensate background, (4.1), are written as follows:

$$\chi_1 = \frac{-8 \left[ 16b^2 r_H^4 + 4a^2(2\alpha^2 b^2 + 1)r_H^2 + a^4 \alpha^4 b^2 \right]}{\left[ -4(b^2 + 6)r_H^2 + a^2(\alpha^2 b^2 + 2) \right]^2}, \quad (\text{B.2a})$$

$$g_1 = \frac{4b^2 r_H^2 - a^2(\alpha^2 b^2 + 2)}{8r_H^2}, \quad (\text{B.2b})$$

$$B_2 = \frac{-6a}{(\alpha^2 b^2 + 2) \left[ -4(b^2 + 6)r_H^2 + a^2(\alpha^2 b^2 + 2) \right]^2} \cdot \left\{ -16b^2 \left[ \frac{1}{3}(\alpha^2 + q^2)b^2 + 2 \left( 2\alpha^2 + q^2 - \frac{1}{3} \right) \right] r_H^4 + \frac{4}{3}a^2 \left[ \alpha^2(2\alpha^2 + q^2)b^4 - (12\alpha^4 - 9\alpha^2 - 2q^2)b^2 + 2 \right] r_H^2 + a^4 \alpha^4 (\alpha^2 b^2 + 2)b^2 \right\}, \quad (\text{B.2c})$$

$$\phi_1 = \frac{4b(4r_H^2 + a^2\alpha^2)}{-4(b^2 + 6)r_H^2 + a^2(\alpha^2 b^2 + 2)}, \quad (\text{B.2d})$$

$$\phi_2 = \frac{-4b}{(\alpha^2 b^2 + 2) \left[ -4(b^2 + 6)r_H^2 + a^2(\alpha^2 b^2 + 2) \right]^3} \left\{ -64(b^2 + 12)(\alpha^2 b^2 + 2)r_H^6 + 16a^2 \left[ \alpha^4(b^4 + 12b^2 + 6)b^2 - \alpha^2 \left( (3q^2 - 2)b^4 + (18q^2 - 37)b^2 - 60 \right) - 2q^2 b^2 - 12q^2 + 10 \right] r_H^4 - 8a^4 \left[ \alpha^6(b^6 + \frac{7b^4}{2} + 9b^2) - \alpha^4 \left( \left( \frac{3q^2}{2} - 4 \right) b^4 - \frac{27b^2}{2} + 6 \right) - \left( 4(q^2 - 1)b^2 - 21 \right) \alpha^2 - 2q^2 \right] r_H^2 + a^6 \alpha^2 (\alpha^2 b^2 + 2) \cdot \left( (\alpha^2 b^2 + 2)^2 + 2\alpha^2(2\alpha^2 b^2 - 1) \right) \right\}. \quad (\text{B.2f})$$

The coefficients of the near horizon expansion of the perturbed field  $C(z)$  are:

$$p_0 = \frac{e^{\frac{\chi_0}{2}}}{(g_1 + 3)r_H}, \quad (\text{B.3a})$$

$$C_1 = \frac{\Gamma}{\Delta}, \quad (\text{B.3b})$$

where,

$$\begin{aligned}
\Gamma = & -2\left(\alpha^2(\chi_1 - 2)b^2 + 2\alpha^2b\phi_1 + 2\chi_1 - 4\right)\omega^2e^{\chi_0} \\
& + 4(g_1 + 3)\left\{\left[2\alpha^2\left(-\omega^2p_0^2 - i\left(\frac{3}{8}\chi_1 + \frac{1}{4}\right)\omega p_0 + \frac{\chi_1}{8}\right)b^2 + i\alpha^2\omega p_0\phi_1(1 - i\omega p_0)b\right.\right. \\
& - 4\omega^2p_0^2 - i\left(\frac{3}{2}\chi_1 + 1\right)\omega p_0 + \frac{\chi_1}{2}\left. \right]g_1 + \left[-9\alpha^2\omega^2p_0^2 - i\left(\frac{9}{4}\chi_1 + 3\right)\alpha^2\omega p_0\right. \\
& + q^2 + \frac{3}{4}\alpha^2\chi_1\left. \right]b^2 + 3i\alpha^2\omega p_0\phi_1(1 - i\omega p_0)b + 18\left(\frac{1}{3} - i\omega p_0\right)\left(\frac{\chi_1}{4} - i\omega p_0\right)\left. \right]r_H^2 \\
& + i\omega(\alpha^2b^2 + 2)\left(\frac{1}{2} - i\omega p_0\right)(g_1 + 3)r_H + \frac{1}{4}a^2(\alpha^2b^2 + 2)^2\left. \right\}, \tag{B.4}
\end{aligned}$$

$$\Delta = 2(\alpha^2b^2 + 2)\left(e^{\chi_0}\omega^2 + r_H^2(g_1 + 3)^2(1 - i\omega p_0)^2\right). \tag{B.5}$$

The cubic equation of  $a^2$  can be written as:

$$\begin{aligned}
0 = & -128(\alpha^2b^2 + 2) \cdot \left(b^6 + \frac{31b^4}{2} + 77b^2 + 114\right)r_H^6 + 96a^2\left[\alpha^4b^8 + \left(\frac{65\alpha^4}{6} + 4\alpha^2\right)b^6\right. \\
& + \left(32\alpha^4 + \left(q^2 + \frac{127}{3}\right)\alpha^2 + 4\right)b^4 + \left(28\alpha^4 + \left(6q^2 + \frac{335}{3}\right)\alpha^2 + \frac{2q^2}{3} + \frac{124}{3}\right)b^2 \\
& + 40\alpha^2 + 4q^2 + \frac{302}{3}\left. \right]r_H^4 - 24a^4\left[\alpha^6b^8 + \left(\frac{37\alpha^6}{6} + 6\alpha^4\right)b^6 + \left(\frac{23\alpha^6}{3} + (q^2 + 35)\alpha^4\right.\right. \\
& + 12\alpha^2\left. \right]b^4 - \left(6\alpha^6 - 31\alpha^4 - \left(\frac{8q^2}{3} + 66\right)\alpha^2 - 8\right)b^2 + 4\alpha^4 + 26\alpha^2 + \frac{4q^2}{3} + \frac{124}{3}\left. \right]r_H^2 \\
& \cdot 2a^6(\alpha^2b^2 + 2) \cdot \left[\alpha^6b^6 + 3\alpha^4\left(\frac{\alpha^2}{2} + 2\right)b^4 - 2\alpha^2(2\alpha^4 - 3\alpha^2 - 6)b^2 + 2\alpha^2(\alpha^2 + 3) + 8\right]. \tag{B.6}
\end{aligned}$$

The DC expansion of the conductivity is:

$$\sigma_{DC}(\omega) = i\sigma_{-1}\omega^{-1} + \sigma_0 + O(\omega), \tag{B.7}$$

$$\begin{aligned}
= & i\left(1 - \frac{2(\alpha^2b^2 + 2)(g_1 + 3)r_H^2}{\Xi}\right)r_H\omega^{-1} + \left(1 - \frac{4p_0(\alpha^2b^2 + 2)(g_1 + 3)r_H^3}{\Xi} + \frac{\Phi}{\Xi^2}\right) \\
& + O(\omega), \tag{B.8}
\end{aligned}$$

where,

$$\Xi = \left[ \left( \alpha^2 + \frac{4q^2}{(\chi_1 + 2)(g_1 + 3)} \right) b^2 + 2 \right] (\chi_1 + 2) (g_1 + 3) r_H^2 + a^2 (\alpha^2 b^2 + 2)^2, \quad (\text{B.9})$$

$$\Phi = 6 \left\{ p_0 \left[ \left( \left( (\chi_1 + 2) g_1 + 3\chi_1 + 8 \right) b - \frac{4}{3} \phi_1 (g_1 + 3) \right) b \alpha^2 + (2\chi_1 + 4) g_1 + 6\chi_1 + 16 \right] r_H - \frac{2}{3} (\alpha^2 b^2 + 2) (g_1 + 3) \right\} (\alpha^2 b^2 + 2) (g_1 + 3) r_H^4. \quad (\text{B.10})$$

- 
- [1] J. Bardeen, L. N. Cooper, and J. R. Schrieffer. Theory of Superconductivity. *Physical Review*, 108:1175–1204, December 1957.
- [2] J. Maldacena. The Large-N Limit of Superconformal Field Theories and Supergravity. *International Journal of Theoretical Physics*, 38:1113–1133, 1999.
- [3] S. S. Gubser, I. R. Klebanov, and A. M. Polyakov. Gauge theory correlators from non-critical string theory. *Physics Letters B*, 428:105–114, May 1998.
- [4] E. Witten. Anti-de Sitter space and holography. *Advances in Theoretical and Mathematical Physics*, 2:253–291, 1998.
- [5] I. R. Klebanov and E. Witten. AdS/CFT correspondence and symmetry breaking. *Nuclear Physics B*, 556:89–114, September 1999.
- [6] O. Aharony, S. S. Gubser, J. Maldacena, H. Ooguri, and Y. Oz. Large N field theories, string theory and gravity. *physrep*, 323:183–386, January 2000.
- [7] S. S. Gubser. Breaking an Abelian gauge symmetry near a black hole horizon. *Phys. Rev. D*, 78(6):065034, September 2008.
- [8] S. A. Hartnoll, C. P. Herzog, and G. T. Horowitz. Building a Holographic Superconductor. *Physical Review Letters*, 101(3):031601, July 2008.
- [9] S. A. Hartnoll, C. P. Herzog, and G. T. Horowitz. Holographic superconductors. *Journal of High Energy Physics*, 12:015, December 2008.
- [10] C. P. Herzog. TOPICAL REVIEW: Lectures on holographic superfluidity and superconductivity. *Journal of Physics A Mathematical General*, 42:343001, August 2009.
- [11] S. Franco, A. García-García, and D. Rodríguez-Gómez. A general class of holographic superconductors. *Journal of High Energy Physics*, 4:92, April 2010.

- [12] F. Aprile and J. G. Russo. Models of holographic superconductivity. *Phys. Rev. D* , 81(2):026009, January 2010.
- [13] G. T. Horowitz. Introduction to Holographic Superconductors. In E. Papantonopoulos, editor, *Lecture Notes in Physics, Berlin Springer Verlag*, volume 828 of *Lecture Notes in Physics, Berlin Springer Verlag*, pages 313–347, 2011.
- [14] G. T. Horowitz and M. M. Roberts. Zero temperature limit of holographic superconductors. *Journal of High Energy Physics*, 11:015, November 2009.
- [15] M. Cadoni, G. D’Appollonio, and P. Pani. Phase transitions between Reissner-Nordstrom and dilatonic black holes in 4D AdS spacetime. *Journal of High Energy Physics*, 3:100, March 2010.
- [16] Y. Liu and Y.-W. Sun. Holographic superconductors from Einstein-Maxwell-Dilaton gravity. *Journal of High Energy Physics*, 7:99, July 2010.
- [17] P. Basu, J. He, A. Mukherjee, M. Rozali, and H.-H. Shieh. Competing holographic orders. *Journal of High Energy Physics*, 10:92, October 2010.
- [18] W.-Y. Wen, M.-S. Wu, and S.-Y. Wu. Holographic model of a two-band superconductor. *Phys. Rev. D* , 89(6):066005, March 2014.
- [19] Y. Peng and Y. Liu. A general holographic metal/superconductor phase transition model. *Journal of High Energy Physics*, 2:82, February 2015.
- [20] Y. Peng and G. Liu. Holographic entanglement entropy in two-order insulator/superconductor transitions. *Physics Letters B*, 767:330–335, April 2017.
- [21] M. Kord Zangeneh, Y. C. Ong, and B. Wang. Entanglement entropy and complexity for one-dimensional holographic superconductors. *Physics Letters B*, 771:235–241, August 2017.
- [22] B. Binaei Ghotbabadi, M. Kord Zangeneh, and A. Sheykhi. One-dimensional backreacting holographic superconductors with exponential nonlinear electrodynamics. *ArXiv e-prints*, April 2018.
- [23] M. Mohammadi, A. Sheykhi, and M. Kord Zangeneh. Analytical and numerical study of backreacting one-dimensional holographic superconductors in the presence of Born-Infeld electrodynamics. *ArXiv e-prints*, May 2018.
- [24] G. T. Horowitz and M. M. Roberts. Holographic superconductors with various condensates. *Phys. Rev. D* , 78(12):126008, December 2008.
- [25] M. Montull, A. Pomarol, and P. J. Silva. Holographic Superconductor Vortices. *Physical*

- Review Letters*, 103(9):091601, August 2009.
- [26] C. P. Herzog. Analytic holographic superconductor. *Phys. Rev. D* , 81(12):126009, June 2010.
- [27] G. T. Horowitz, J. E. Santos, and B. Way. Holographic Josephson Junctions. *Physical Review Letters*, 106(22):221601, June 2011.
- [28] A. Salvio. Holographic superfluids and superconductors in dilaton-gravity. *Journal of High Energy Physics*, 9:134, September 2012.
- [29] H. B. Zeng, Y. Tian, Z. Y. Fan, and C.-M. Chen. Nonlinear transport in a two dimensional holographic superconductor. *Phys. Rev. D* , 93(12):121901, June 2016.
- [30] L. Yin, H.-c. Ren, T. K. Lee, and D. Hou. Momentum analyticity of transverse polarization tensor in the normal phase of a holographic superconductor. *Journal of High Energy Physics*, 8:116, August 2016.
- [31] T.-S. Huang and W.-Y. Wen. Holographic Model of Dual Superconductor for Quark Confinement. *ArXiv e-prints*, July 2016.
- [32] K.-Y. Kim and C. Niu. Homes' law in Holographic Superconductor with Q-lattices. *ArXiv e-prints*, August 2016.
- [33] A. Sheykhi, F. Shamsi, and S. Davatolhagh. The upper critical magnetic field of holographic superconductor with conformally invariant Power-Maxwell electrodynamics. *Canadian Journal of Physics*, 95:450–456, May 2017.
- [34] B. Pourhassan and M. M. Bagheri-Mohagheghi. Holographic superconductor in a deformed four-dimensional STU model. *European Physical Journal C*, 77:759, November 2017.
- [35] Y. Ling, P. Liu, and J.-P. Wu. Note on the butterfly effect in holographic superconductor models. *Physics Letters B*, 768:288–291, May 2017.
- [36] G. Alkac, S. Chakraborty, and P. Chaturvedi. Holographic P -wave superconductors in 1 +1 dimensions. *Phys. Rev. D* , 96(8):086001, October 2017.
- [37] H. B. Zeng, Y. Tian, Z. Fan, and C.-M. Chen. Nonlinear conductivity of a holographic superconductor under constant electric field. *Phys. Rev. D* , 95(4):046014, February 2017.
- [38] O. DeWolfe, O. Henriksson, and C. Wu. A holographic model for pseudogap in BCS-BEC crossover (I): Pairing fluctuations, double-trace deformation and dynamics of bulk bosonic fluid. *Annals of Physics*, 387:75–120, December 2017.
- [39] Y.-F. Cai, S. Lin, J. Liu, and J.-R. Sun. Holographic Preheating: Quasi-Normal Modes and Holographic Renormalization. *ArXiv e-prints*, December 2016.

- [40] J. Erdmenger, M. Flory, M.-N. Newrzella, M. Strydom, and J. M. S. Wu. Quantum quenches in a holographic Kondo model. *Journal of High Energy Physics*, 4:45, April 2017.
- [41] S. A. Hartnoll, A. Lucas, and S. Sachdev. Holographic quantum matter. *ArXiv e-prints*, December 2016.
- [42] M. Natsuume and T. Okamura. Kibble-Zurek scaling in holography. *Phys. Rev. D* , 95(10):106009, May 2017.
- [43] A. Gorsky, E. Gubankova, R. Meyer, and A. Zayakin. S -duality for holographic p -wave superconductors. *Phys. Rev. D* , 96(10):106010, November 2017.
- [44] Z.-H. Li, Y.-C. Fu, and Z.-Y. Nie. Competing s-wave orders from Einstein-Gauss-Bonnet gravity. *Physics Letters B*, 776:115–123, January 2018.
- [45] A. Gorsky and F. Popov. On magnetic and vortical susceptibilities of the Cooper condensate. *Physics Letters B*, 774:135–138, November 2017.
- [46] A. Kundu. Flavours and infra-red instability in holography. *Journal of High Energy Physics*, 11:101, November 2017.
- [47] J.-P. Wu and P. Liu. Holographic superconductivity from higher derivative theory. *Physics Letters B*, 774:527–532, November 2017.
- [48] M. Kord Zangeneh, S. S. Hashemi, A. Dehyadegari, A. Sheykhi, and B. Wang. Optical properties of Born-Infeld-dilaton-Lifshitz holographic superconductors. *ArXiv e-prints*, October 2017.
- [49] A. Sheykhi, A. Ghazanfari, and A. Dehyadegari. Holographic conductivity of holographic superconductors with higher-order corrections. *European Physical Journal C*, 78:159, February 2018.
- [50] D. Parai, D. Ghorai, and S. Gangopadhyay. Noncommutative effects of charged black hole on holographic superconductors. *ArXiv e-prints*, January 2018.
- [51] S. I. Kruglov. Holographic superconductor with nonlinear arcsin-electrodynamics. *ArXiv e-prints*, January 2018.
- [52] A. Sheykhi, D. Hashemi Asl, and A. Dehyadegari. Conductivity of higher dimensional holographic superconductors with nonlinear electrodynamics. *Physics Letters B*, 781:139–154, June 2018.
- [53] D. Wen, H. Yu, Q. Pan, K. Lin, and W.-L. Qian. A Maxwell-vector p-wave holographic superconductor in a particular background AdS black hole metric. *Nuclear Physics B*, 930:255–

269, May 2018.

- [54] J. Cheng, Q. Pan, H. Yu, and J. Jing. Refractive index in generalized superconductors with Born-Infeld electrodynamics. *European Physical Journal C*, 78:239, March 2018.
- [55] T. Ishii and K. Murata. Floquet superconductor in holography. *ArXiv e-prints*, April 2018.
- [56] N. Iqbal, H. Liu, M. Mezei, and Q. Si. Quantum phase transitions in holographic models of magnetism and superconductors. *Phys. Rev. D*, 82(4):045002, August 2010.
- [57] M. Rogatko and K. I. Wysokinski. Condensate flow in holographic models in the presence of dark matter. *Journal of High Energy Physics*, 10:152, October 2016.
- [58] Y. Peng. Studies of a general flat space/boson star transition model in a box through a language similar to holographic superconductors. *Journal of High Energy Physics*, 7:42, July 2017.
- [59] Y. Peng, B. Wang, and Y. Liu. On the thermodynamics of the black hole and hairy black hole transitions in the asymptotically flat spacetime with a box. *European Physical Journal C*, 78:176, March 2018.
- [60] T. Andrade, A. Krikun, K. Schalm, and J. Zaanen. Doping the holographic Mott insulator. *ArXiv e-prints*, October 2017.
- [61] Y. Peng. A general quasi-local flat space/boson star transition model and holography. *ArXiv e-prints*, October 2017.
- [62] Y. Ling, P. Liu, J.-P. Wu, and M.-H. Wu. Holographic superconductor on a novel insulator. *Chinese Physics C*, 42(1):013106, January 2018.
- [63] G. Filios, P. A. González, X.-M. Kuang, E. Papantonopoulos, and Y. Vásquez. Spontaneous Momentum Dissipation and Coexistence of Phases in Holographic Horndeski Theory. *arXiv e-prints*, August 2018.
- [64] O. Domènech, M. Montull, A. Pomarol, A. Salvio, and P. J. Silva. Emergent gauge fields in holographic superconductors. *Journal of High Energy Physics*, 8:33, August 2010.
- [65] M. Montull, O. Pujolàs, A. Salvio, and P. J. Silva. Flux Periodicities and Quantum Hair on Holographic Superconductors. *Physical Review Letters*, 107(18):181601, October 2011.
- [66] M. Montull, O. Pujolàs, A. Salvio, and P. J. Silva. Magnetic response in the holographic insulator/superconductor transition. *Journal of High Energy Physics*, 4:135, April 2012.
- [67] A. Salvio. Transitions in dilaton holography with global or local symmetries. *Journal of High Energy Physics*, 3:136, March 2013.



- [68] A. Dey, S. Mahapatra, and T. Sarkar. Generalized holographic superconductors with higher derivative couplings. *Journal of High Energy Physics*, 6:147, June 2014.
- [69] S. Mahapatra, P. Phukon, and T. Sarkar. Generalized superconductors and holographic optics. *Journal of High Energy Physics*, 1:135, January 2014.
- [70] S. Mahapatra. Generalized superconductors and holographic optics. Part II. *Journal of High Energy Physics*, 1:148, January 2015.
- [71] A. Sheykhi and F. Shaker. Analytical study of holographic superconductor in Born-Infeld electrodynamics with backreaction. *Physics Letters B*, 754:281–287, March 2016.
- [72] A. Sheykhi and F. Shaker. Effects of backreaction and exponential nonlinear electrodynamics on the holographic superconductors. *International Journal of Modern Physics D*, 26:1750050, 2017.
- [73] H. R. Salahi, A. Sheykhi, and A. Montakhab. Effects of backreaction on power-Maxwell holographic superconductors in Gauss-Bonnet gravity. *European Physical Journal C*, 76:575, October 2016.
- [74] Z. Sherkatghanad, B. Mirza, and F. Lalehgani Dezaki. Exponential nonlinear electrodynamics and backreaction effects on holographic superconductor in the Lifshitz black hole background. *International Journal of Modern Physics D*, 27:1750175, 2018.
- [75] D. Ghorai and S. Gangopadhyay. Conductivity of holographic superconductors in Born-Infeld electrodynamics. *ArXiv e-prints*, October 2017.
- [76] A. Amoretti, D. Areán, B. Goutéraux, and D. Musso. DC resistivity of quantum critical, charge density wave states from gauge-gravity duality. *ArXiv e-prints*, December 2017.
- [77] R. Gregory, S. Kanno, and J. Soda. Holographic superconductors with higher curvature corrections. *Journal of High Energy Physics*, 10:010, October 2009.
- [78] C. Chen and M. Wu. An Analytic Analysis of Phase Transitions in Holographic Superconductors. *Progress of Theoretical Physics*, 126:387–395, September 2011.
- [79] X. Ge and H. Leng. Analytical Calculation on Critical Magnetic Field in Holographic Superconductors with Backreaction. *Progress of Theoretical Physics*, 128:1211–1228, December 2012.
- [80] A. J. Nurbagambetov. Analytical approach to phase transitions in rotating and non-rotating 2D holographic superconductors. *ArXiv e-prints*, July 2011.
- [81] D. Roychowdhury. Effect of external magnetic field on holographic superconductors in pres-

- ence of nonlinear corrections. *Phys. Rev. D* , 86(10):106009, November 2012.
- [82] W.-H. Huang. Analytic Study of First-Order Phase Transition in Holographic Superconductor and Superfluid. *International Journal of Modern Physics A*, 28:1350140, October 2013.
- [83] A. Sheykhi and F. Shamsi. Holographic Superconductors with Logarithmic Nonlinear Electrodynamics in an External Magnetic Field. *International Journal of Theoretical Physics*, 56:916–930, March 2017.
- [84] Y. Ling and X. Zheng. Holographic superconductor with momentum relaxation and Weyl correction. *Nuclear Physics B*, 917:1–18, April 2017.
- [85] D. Ghorai and S. Gangopadhyay. Non-linear effects on the holographic free energy and thermodynamic geometry. *EPL (Europhysics Letters)*, 118:31001, May 2017.
- [86] S. R. Das, M. Fujita, and B. S. Kim. Holographic entanglement entropy of a 1 + 1 dimensional p-wave superconductor. *Journal of High Energy Physics*, 9:16, September 2017.
- [87] S. Pal and S. Gangopadhyay. Noncommutative effects on holographic superconductors with power Maxwell electrodynamics. *Annals of Physics*, 388:472–484, January 2018.